BMC Plant Biology

RESEARCH

Open Access

Genome-wide identification of MGT gene family in soybean (*Glycine max*) and their expression analyses under magnesium stress conditions

Ammar Anwar[1], Junaid Akhtar[1], Saba Aleem[2], Maida Aleem[3], Muhammad Khuram Razzaq[4], Saud Alamri[5], Qasim Raza[1,6], Iram Sharif[7], Arooj Iftikhar[8], Shehreen Naseer[1], Zaheer Ahmed[1], Iqrar Ahmed Rana[9], Waheed Arshad[2], Muhammad Imran Khan[2], Javaid Akhter Bhat[10], Muqadas Aleem[1,11*], Abdel-Rhman Z. Gaafar[5] and Mohamed S. Hodhod[12]

Abstract

Background Magnesium (Mg) is essential for plant growth and development and plays critical roles in physiological and biochemical processes. Mg deficiency adversely affects growth of plants by limiting shoot and root development, disturbing the structure and membranes of the grana, reducing photosynthesis efficiency, and lowering net CO_2 assimilation. The MGT (Magnesium transporter) family is responsible for the absorption and transportation of magnesium in plants. Although the MGT family has been identified in different plant species, research regarding the soybean MGT genes is limited.

Results In the current study, a total of 39 MGT genes distributed on 17 different chromosomes were identified in soybean. Phylogenetic analysis classified *GmMGTs* into three subgroups, NIPA, MRS2/MGT, and CorA, which showed little homology with MGTs of *Arabidopsis thaliana* and *Oryza sativa* members and clustered tightly with *GmMGTs*. Gene structure and conserved motif analysis also confirmed similar grouping in *GmMGTs*. The expansion of the *GmMGT* members in NIPA and MRS2/MGT was predicted, while CorA was identified as the most conserved group in *G. max*. Segmental duplication under purifying selection pressure was identified as the major driving force in the expansion of MGTs in soybean. *GmMGTs* showed diverse tissue-specific and stress-response expression patterns due to the presence of stress-related cis-regulatory elements in their promoter regions. Under Mg-deficiency and surplus stress conditions, a decrease in root length, shoot length, and root and shoot fresh as well dry weight in susceptible genotypes showed the variegated expression of MGTs in soybean genotypes. Furthermore, the upregulation of *GmMGT2* and *GmMGT29* in tolerant genotypes in response to Mg-deficiency as well as surplus stress conditions in leaves suggested the essential role of *GmMGT* genes in the absorption and transportation of Mg in soybean leaves.

Conclusion This study presents a comprehensive analysis of the MGT gene family in soybean, providing insights into their evolutionary relationships, gene classification, protein structures, and expression patterns under both Mg deficiency and Mg surplus conditions.

Keywords Magnesium transporter, *Glycine max*, MRS/MGT, NIPA, CorA, Mg deficient, Mg surplus

*Correspondence:
Muqadas Aleem
muqadas.aleem@uaf.edu.pk
Full list of author information is available at the end of the article

© The Author(s) 2025. **Open Access** This article is licensed under a Creative Commons Attribution-NonCommercial-NoDerivatives 4.0 International License, which permits any non-commercial use, sharing, distribution and reproduction in any medium or format, as long as you give appropriate credit to the original author(s) and the source, provide a link to the Creative Commons licence, and indicate if you modified the licensed material. You do not have permission under this licence to share adapted material derived from this article or parts of it. The images or other third party material in this article are included in the article's Creative Commons licence, unless indicated otherwise in a credit line to the material. If material is not included in the article's Creative Commons licence and your intended use is not permitted by statutory regulation or exceeds the permitted use, you will need to obtain permission directly from the copyright holder. To view a copy of this licence, visit http://creativecommons.org/licenses/by-nc-nd/4.0/.

Content courtesy of Springer Nature, terms of use apply. Rights reserved.

Background

Magnesium, the second most prevalent intracellular cation in plants, is crucial for the growth and development of plants [1]. Mg is involved in different cellular functions, i.e., photosynthesis, enzyme activation, and the synthesis of nucleic acids and proteins [2, 3]. Magnesium's high mobility within plants is a key reason for the substantial impact of magnesium deficiencies on plant growth and development.. Magnesium deficiency results into various symptoms, including chlorosis of mature leaf interveinal areas and a decrease in root and shoot growth. This also lowers the photosynthetic efficiency by disturbing the structure and membrane of the grana. Mg deficiency also has a detrimental effect on the allocation of carbon to sink organs and hinders the growth of plant roots, which has a negative influence on crop yield and quality [4–6]. A meta-analysis suggested that applying a reasonable amount of magnesium may increase the yield upto 8.5% in cereals, fruits and vegetables etc [7].

Based on sequence conservation, three distinct forms of Mg transporters i.e., Mgt A/B, Cor A (Cobalt (Co2 +) resistant A), and MgtE have been discovered in prokaryotes [8]. The CorA-type proteins have been identified in a variety of organisms in the past i.e. yeast, plants, and even animals [9, 10]. The MRS2/MGT gene family, initially identified as homologues to Cor A type in plants, was first discovered in Arabidopsis and later in rice. Currently, extensive analysis have been undergone in various crops [11–13]. The identification and characterization of the MGT family in maize [14], *Brassica napus* [15], sugarcane [16], wheat [17], banana [18], tomato [19], *Triticum turgidum* and *Camelina sativa* [20] have been carried out in the last decade.

Investigating MGTs in soybean and exploring their regulatory mechanisms in response to Mg stress also holds great significance. This is particularly interesting because soybean (*Glycine max*) is a crucial annual oilseed crop [21]. Being nutrient-rich, it has economic value and very large utility in agriculture as well as in industry. Among all plant-based protein sources, soybean protein has good protein content and high digestibility, making it a vital constituent of poultry and livestock feed [22]. Mg deficiency negatively impacts soybean growth by restricting both shoot and root development, which, in turn, weakens vascular tissues, hampering water and nutrient uptake [23]. Experiments have shown that Mg application improves soybean root, shoot, stem, and pod biomass [24]. However, most of these studies focused on phenotypic traits to enhance growth, nodulation, and yield in soybean [23–25]. However, knowledge of the regulatory mechanisms involved in soybean responses to Mg stress, particularly the role of the MGT family, are still not well understood. Therefore, this study aimed to expand our understanding of MGTs in soybean by utilizing the recently sequenced *G. max* genome. By doing so, we successfully identified the MGTs in soybean (referred to as *GmMGTs*) and investigated their evolutionary relationships and potential functions through phylogenetic analysis, comparative genomics, and gene expression pattern analysis.

Results

Identification and characterization of MGT family members in G. max, A. thaliana, and O. sativa

A systematic approach was used to explore the MGT genes of *G. max, A. thaliana,* and *O. sativa* in publicly available databases. Initially, 27 *MGT* genes in Arabidopsis and 20 MGT genes in *O. sativa* were retrieved. Then these gene sequences were blasted against the soybean genome in the Phytozome search tool and a total of 52 MGT sequences were retrieved in soybean. Further, NCBI CDD search tool was used for the confirmation of MGT domains e.g., MGT/MRS, NIPA, and CorA. After the removal of short sequences (less than 150 bp), 24 *MGT* genes in *A. thaliana*, 20 in *O. sativa,* and *39* in *G. max* were identified. The nomenclature of *G. max* genes was set as *GmMGT*, followed by the continuous number that represents the continuous position of the genes on chromosomes from 1 to 20. For example, *GmMGT1* refers to the first MGT gene located on chromosome 1, *GmMGT2* is the second gene on chromosome 2, and *GmMGT3* represents the third gene on chromosome 2 in *G. max*.

Detailed information on the MGT genes in soybean, with their Phytozome gene ID, rename ID, chromosome number, strand orientation, gene length, CDS length, protein size, molecular weight, isoelectric points, and sub-cellular localization is presented in Table 1. In *G. max* the MGTs gene length ranged from 381 bp (base pairs) in *GmMGT16* to 1668 bp (*GmMGT34*). The protein size of *G. max* ranged from 127 (*GmMGT3*, *GmMGT33*) to 556 amino acids (*GmMGT24*), the molecular weight ranged from 14.1 kDa (*GmMGT16*) to 62.3 kDa (*GmMGT34*) and their isoelectric point (PI) varied from 4.47 (*GmMGT21*) to 9.91 (*GmMGT14*). Further, most of the *GmMGTs* were predicted in the plasma membrane and a few genes were present in cytoplasm and nuclear. i.e., *GmMGT6, GmMGT*10, *GmMGT*18, *GmMGT*28, *GmMGT*29, and *GmMGT*39 were present in Nucleus, while *GmMGT*1, *GmMGT*19, *GmMGT*20, *GmMGT*26, *GmMGT*27, *GmMGT*34 and *GmMGT*38 were predicted in cytoplasm (Table 1).

Content courtesy of Springer Nature, terms of use apply. Rights reserved.

Table 1 Identified MGT genes of *G. max,* including their phytozome ID, rename ID, rename ID, chromosome number, strand orientation, protein size, molecular weight, PI and Sub-cellular localization of the genes

Phytozome ID	Gene Name	Gene Rename	Chr. No	Strand Ori	Start Point	End Point	Gene length	Protein Size	Mw (kDa)	PI	Sub-cellular localization
glyma.Wm82.gnm4.ann1.Glyma.01G242000	*Glyma.01G242000*	*GmMGT1*	*1*	+	*56,560,550*	*56,563,303*	*1182*	*363*	44.0	*4.9*	*Cytoplasmic*
glyma.Wm82.gnm4.ann1.Glyma.02G068000	*Glyma.02G068000*	*GmMGT2*	*2*	+	*5,991,168*	*5,997,336*	*1332*	*346*	37.5	*9.88*	*Plasma Membrane*
glyma.Wm82.gnm4.ann1.Glyma.02G117100	*Glyma.02G117100*	*GmMGT3*	*2*	-	*11,400,594*	*11,409,016*	*1245*	*127*	46.4	*5.13*	*Plasma Membrane*
glyma.Wm82.gnm4.ann1.Glyma.02G280800	*Glyma.02G280800*	*GmMGT4*	*2*	-	*46,313,390*	*46,318,217*	*1050*	*412*	37.9	*8.16*	*Plasma Membrane*
glyma.Wm82.gnm4.ann1.Glyma.02G285600	*Glyma.02G285600*	*GmMGT5*	*2*	+	*46,655,327*	*46,660,517*	*1629*	*451*	62.1	*6.39*	*Plasma Membrane*
glyma.Wm82.gnm4.ann1.Glyma.03G159400	*Glyma.03G159400*	*GmMGT6*	*3*	+	*37,457,902*	*37,462,063*	*1167*	*463*	43.7	*5.1*	*Nuclear*
glyma.Wm82.gnm4.ann1.Glyma.04G005200	*Glyma.04G005200*	*GmMGT7*	*4*	-	*433,402*	*436,407*	*1005*	*230*	36.3	*6.7*	*Plasma Membrane*
glyma.Wm82.gnm4.ann1.Glyma.04G052700	*Glyma.04G052700*	*GmMGT8*	*4*	-	*4,270,522*	*4,275,064*	*4543*	*321*	37.5	*9.88*	*Plasma Membrane*
glyma.Wm82.gnm4.ann1.Glyma.05G153000	*Glyma.05G153000*	*GmMGT9*	*5*	+	*34,674,924*	*34,679,741*	*966*	*391*	35.1	*8.29*	*Plasma Membrane*
glyma.Wm82.gnm4.ann1.Glyma.05G168200	*Glyma.05G168200*	*GmMGT10*	*5*	-	*35,871,339*	*35,874,984*	*1356*	*400*	50.7	*5.87*	*Nuclear and Cytoplasmic*
glyma.Wm82.gnm4.ann1.Glyma.05G196000	*Glyma.05G196000*	*GmMGT11*	*5*	-	*38,018,002*	*38,019,219*	*495*	*181*	18.5	*7.02*	*Plasma Membrane Chloroplast Nuclear*
glyma.Wm82.gnm4.ann1.Glyma.05G196600	*Glyma.05G196600*	*GmMGT12*	*5*	-	*38,081,436*	*38,085,776*	*1036*	*327*	37.2	*6.58*	*Plasma Membrane*
glyma.Wm82.gnm4.ann1.Glyma.06G005000	*Glyma.06G005000*	*GmMGT13*	*6*	-	*424,493*	*428,218*	*1089*	*374*	39.3	*7.07*	*Plasma Membrane*
glyma.Wm82.gnm4.ann1.Glyma.06G053100	*Glyma.06G053100*	*GmMGT14*	*6*	-	*4,017,860*	*4,022,498*	*4639*	*345*	36.9	*9.91*	*Plasma Membrane*
glyma.Wm82.gnm4.ann1.Glyma.06G159100	*Glyma.06G159100*	*GmMGT15*	*6*	-	*13,102,705*	*13,106,565*	*1038*	*357*	37.6	*6.88*	*Plasma Membrane*
glyma.Wm82.gnm4.ann1.Glyma.06G208700	*Glyma.06G208700*	*GmMGT16*	*6*	-	*20,398,863*	*20,400,310*	*381*	*348*	14.1	*9*	*Plasma Membrane*
glyma.Wm82.gnm4.ann1.Glyma.08G003600	*Glyma.08G003600*	*GmMGT17*	*8*	-	*269,359*	*271,945*	*1236*	*458*	46.6	*4.89*	*Plasma Membrane Cytoplasmic Nuclear*
glyma.Wm82.gnm4.ann1.Glyma.08G126600	*Glyma.08G126600*	*GmMGT18*	*8*	-	*9,751,314*	*9,754,613*	*1353*	*468*	50.6	*5.82*	*Nuclear*
glyma.Wm82.gnm4.ann1.Glyma.10G180200	*Glyma.10G180200*	*GmMGT19*	*10*	+	*41,387,259*	*41,392,378*	*1173*	*441*	54.3	*5*	*Cytoplasmic*

Content courtesy of Springer Nature, terms of use apply. Rights reserved.

Table 1 (continued)

Phytozome ID	Gene Name	Gene Rename	Chr. No	Strand Ori	Start Point	End Point	Gene length	Protein Size	Mw (kDa)	PI	Sub-cellular localization
glyma.Wm82.gnm4.ann1.Glyma.11G002200	*Glyma.11G002200*	*GmMGT20*	*11*	-	*115,811*	*118,160*	*1200*	*350*	44.5	*4.72*	*Cytoplasmic*
glyma.Wm82.gnm4.ann1.Glyma.11G105300	*Glyma.11G105300*	*GmMGT21*	*11*	+	*8,004,678*	*8,006,385*	*543*	*350*	20.1	*4.47*	*Plasma Membrane*
glyma.Wm82.gnm4.ann1.Glyma.11G255400	*Glyma.11G255400*	*GmMGT22*	*11*	+	*34,547,190*	*34,550,103*	*981*	*441*	35.4	*8.36*	*Plasma Membrane*
glyma.Wm82.gnm4.ann1.Glyma.12G030100	*Glyma.12G030100*	*GmMGT23*	*12*	+	*2,250,621*	*2,254,011*	*1122*	*310*	40.9	*7.63*	*Plasma Membrane*
glyma.Wm82.gnm4.ann1.Glyma.12G159000	*Glyma.12G159000*	*GmMGT24*	*12*	+	*27,382,543*	*27,399,576*	*1071*	*556*	39.4	*6.59*	*Plasma Membrane*
glyma.Wm82.gnm4.ann1.Glyma.12G168000	*Glyma.12G168000*	*GmMGT25*	*12*	+	*32,279,586*	*32,285,662*	*1053*	*348*	38.1	*7.04*	*Plasma Membrane*
glyma.Wm82.gnm4.ann1.Glyma.12G180000	*Glyma.12G180000*	*GmMGT26*	*12*	-	*34,047,574*	*34,053,748*	*1374*	*444*	51.1	*5.47*	*Cytoplasmic and Nuclear*
glyma.Wm82.gnm4.ann1.Glyma.13G254800	*Glyma.13G254800*	*GmMGT27*	*13*	+	*36,053,618*	*36,059,593*	*1404*	*344*	53.1	*8.77*	*Cytoplasmic*
glyma.Wm82.gnm4.ann1.Glyma.13G320800	*Glyma.13G320800*	*GmMGT28*	*13*	+	*41,504,465*	*41,510,677*	*1371*	*162*	50.9	*5.67*	*Nuclear and Cytoplasmic*
glyma.Wm82.gnm4.ann1.Glyma.13G368400	*Glyma.13G368400*	*GmMGT29*	*13*	-	*45,393,906*	*45,398,210*	*1248*	*389*	46.4	*4.66*	*Nuclear, Cytoplasmic*
glyma.Wm82.gnm4.ann1.Glyma.13G370900	*Glyma.13G370900*	*GmMGT30*	*13*	-	*45,618,183*	*45,622,734*	*1332*	*396*	50.4	*5.13*	*Plasma Membrane*
glyma.Wm82.gnm4.ann1.Glyma.14G033700	*Glyma.14G033700*	*GmMGT31*	*14*	+	*2,472,243*	*2,477,533*	*1050*	*363*	37.8	*8.11*	*Plasma Membrane*
glyma.Wm82.gnm4.ann1.Glyma.14G097400	*Glyma.14G097400*	*GmMGT32*	*14*	-	*9,185,438*	*9,190,929*	*1050*	*346*	37.9	*9.41*	*Plasma Membrane*
glyma.Wm82.gnm4.ann1.Glyma.15G002700	*Glyma.15G002700*	*GmMGT33*	*15*	+	*256,675*	*262,020*	*1332*	*127*	50.4	*5.18*	*Plasma Membrane*
glyma.Wm82.gnm4.ann1.Glyma.15G125900	*Glyma.15G125900*	*GmMGT34*	*15*	-	*9,970,216*	*9,977,246*	*1668*	*451*	62.3	*6.16*	*Cytoplasmic*
glyma.Wm82.gnm4.ann1.Glyma.16G003900	*Glyma.16G003900*	*GmMGT35*	*16*	+	*218,321*	*224,654*	*1044*	*463*	37.9	*7.04*	*Plasma Membrane*
glyma.Wm82.gnm4.ann1.Glyma.16G149500	*Glyma.16G149500*	*GmMGT36*	*16*	+	*31,012,408*	*31,020,015*	*1332*	*230*	49.0	*8.48*	*Plasma Membrane*

Content courtesy of Springer Nature, terms of use apply. Rights reserved.

Table 1 (continued)

Phytozome ID	Gene Name	Gene Rename	Chr. No	Strand Ori	Start Point	End Point	Gene length	Protein Size	Mw (kDa)	PI	Sub-cellular localization
glyma.Wm82.gnm4.ann1.Glyma.17G227100	*Glyma.17G227100*	*GmMGT37*	*17*	+	*38,175,388*	*38,181,189*	*1032*	*391*	37.1	*9.61*	*Plasma Membrane*
glyma.Wm82.gnm4.ann1.Glyma.19G161600	*Glyma.19G161600*	*GmMGT38*	*19*	+	*42,231,749*	*42,235,587*	*1167*	*181*	43.5	*5.11*	*Cytoplasmic, Nuclear*
glyma.Wm82.gnm4.ann1.Glyma.20G210300	*Glyma.20G210300*	*GmMGT39*	*20*	-	*44,633,804*	*44,638,663*	*1188*	*327*	44.0	*4.94*	*Nuclear, Cytoplasmic*

Content courtesy of Springer Nature, terms of use apply. Rights reserved.

Phylogenetic Tree, Gene Structure, Motif, and Protein Structure Analysis

To reveal the evolutionary relationship of MGTs in *G. max*, a phylogenetic tree was constructed. The phylogenetic tree exhibited a distribution of MGTs in three distinct groups based on conserved domains e.g., MRS 2/MGT, NIPA, and CorA (Fig. 1A). The *GmMGTs* exon–intron arrangement showed a similar pattern of similarity as in the phylogenetic tree. MGT genes belonging to different groups like MRS, NIPA, and CoreA showed significant variation in exon and intron number and arrangement e.g., *GmMGT25, GmMGT27,* and *GmMGT10.* However, genes lying near each other within a group showed a similar structural pattern with a similar number of exons and introns e.g., *GmMGT25* and *GmMGT35* (Fig. 1B). Among *GmMGT*s proteins, 8 diverse conserved motifs were recognized. These motifs also showed similarities in the distribution and grouping according to the phylogenetic tree. Five conserved motifs were identified in the NIPA group, while in MRS/MGT three conserved motifs were found. However, in the CorA group, no conserved motif was found. The presence of conserved motifs within a group e.g., MRS/MGT shows the similar functions of proteins (Fig. 1C).

The 3-D structures of *GmMGTs* of NIPA, MRS2, and CorA proteins, showed conserved domain presence in each of them. The conserved domains exhibited a characteristic three-dimensional framework consisting of multiple parallel α-helices. Notably, a significant similarity was observed in the metal ion and Mg2 + binding sites, along with the catalytic regions of the proteins. Nevertheless, variations in the protein sequences were observed within and among different groups. Among the MRS/MGT group, a few proteins exhibited similar 3D structures, while most of the genes displayed diverse structures. Likewise, variations in protein structure were observed within the NIPA and CorA members. The diverse protein structures in these cases likely reflect their distinct roles in transmembrane transport processes, adapting to different environmental conditions (Fig. 2).

Chromosome mapping and duplication of MGTs in soybean

To understand the chromosomal location and distribution of *GmMGT* genes in soybean, chromosomal mapping was performed. 39 genes of *GmMGT* were unevenly positioned on 17 chromosomes of the soybean genome. Chromosome numbers 2, 5, 6, 12, and 13 have the highest number of MGT genes. In contrast, chromosomes 1, 10, 17, 19, and 20 have only 1 gene while no gene is present on chromosomes 7, 9, and 18 (Fig. 3).

For a better understanding of the evolution of MGT, the gene duplication events in MGTs of *G. max* were explored. There were multiple duplicate copies of MGT genes in the soybean genome because of two whole-genome duplication events and one whole-genome triplication, and approximately 75% of paralogues were found in soybean. Our results suggested that approximately 14 segmental duplication events occurred in 39 MGT genes of soybean (Table 2).

Estimation of divergence time for homologs GmMGT gene pairs

To assess the selection pressure on MGT PGPs, Ka and Ks substitution rate per site per year was calculated. For *GmMGT* PGPs, the Ka/Ks varied from 0.11 to 0.46 indicating that all PGPs of *GmMGT* genes have evolved through purifying selection pressure. $T = Ks/2\lambda$ was used to measure the divergence time. The approximate divergence time between the duplication events showed that duplication events occurred between 6.36 and 104.64 MYA as shown in Table 2. Duplication of *GmMGT22/GmMGT13* occurred almost 104.64 MYA ago, which was far from the duplication of other PGPs of MGTs. However, the most recent duplication event among the MGT gene pairs in *G. max* occurred between *GmMGT4* and *GmMGT29,* approximately 6.36 million years ago.

Putative cis-acting regulatory elements in GmMGTs

All the identified cis-elements in *GmMGTs* are categorized into three groups: biotic stress-responsive elements, phytohormone regulating elements, and elements involved in plant growth and development. A wide range of light-responsive elements including the GT1-motif, AE-box, AT1-motif, chs-CMA1a, TCCC-motif, GATA-motif, and many more explained in Table 3, have been identified in *GmMGTs* promoter region. TC-rich repeat elements participate in stress response and the defense mechanism of the plant was also identified. In *G. max,* multiple phytohormones are also identified in the MGT promoter, suggesting that *GmMGTs* expression is modulated by various phytohormones including MeJA, salicylic acid, gibberellin acid, abscisic acid, and auxin-responsive elements. Four elements that fall in the plant growth and development category i.e., meristem expression element (CAT-box), endosperm regulating element (GCN4-motif), circadian element, and zein metabolism-regulating element (O2-site) were also identified. Detailed description of cis elements of each *GmMGT* gene is presented in Additional file 1.

Comparative Relationship of G. max MGTs with Other Model Plants

An neighbor-joining (NJ) tree was constructed using *MGT* protein sequences of *A. thaliana*, *O. sativa, and G. max* to study the comparative evolutionary relationship

Content courtesy of Springer Nature, terms of use apply. Rights reserved.

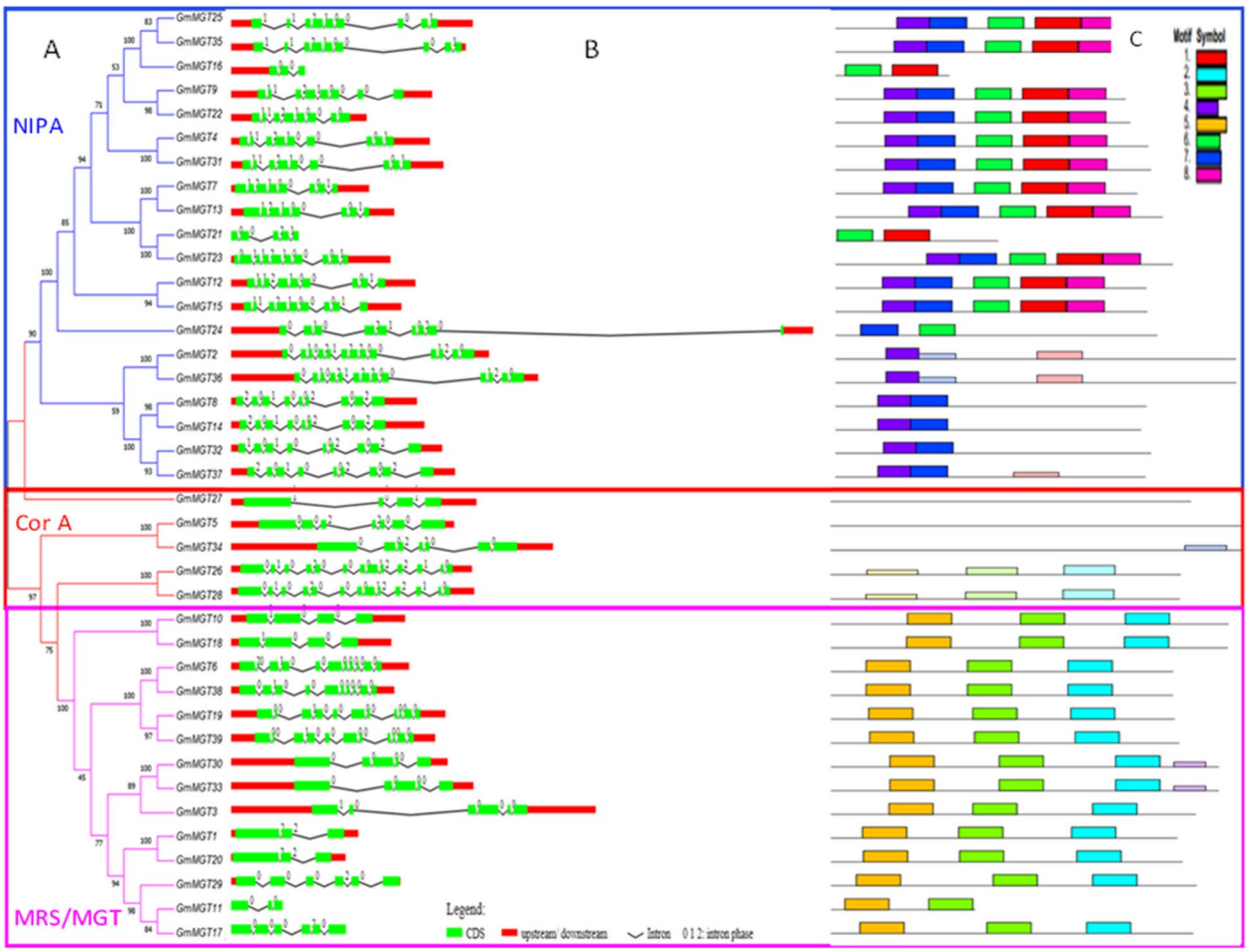

Fig. 1 Phylogenetic relationship, exon–intron distribution/gene structure and conserved motifs in MGT gene family in *G. max*. **A** The phylogenetic tree of the MGT gene family classified into three clades/groups highlighted with different colored boxes. **B** The untranslated region (UTR), with intron and exon distribution represented by a red box, green rectangles and black hats, respectively. **C** Conserved motifs in MGT genes. Each motif is presented by a particular color

among them. MGTs of all selected spp. were clustered into three groups of *MGTs* (MRS 2/MGT, NIPA, and CorA). Eighty-three magnesium transporter genes were identified in these species. Thirty-three genes were classified in group MRS 2/MGT, 39 in NIPA, and 11 in Group CorA. Furthermore, there was no equal representation of the MGTs from the three species within the group. Group MRS contains 10, NIPA contains 09, and CorA contains 5 *MGTs* of *A. thaliana*, while 14, 20, and 5 MGTs of *G. max*, were present in each group and 8, 10 and 1 of the *OsMGTs* respectively. *G. max* MGTs showed tight clustering with each other rather than with *A. thaliana* and *O. sativa* (Fig. 4).

Synteny analysis of GmMGTs with Glycine soja MGTs

A dual synteny plot was constructed between *G. max* and *Glycine soja* a wild soybean species. A total of 29 OGPs were found showing that these OGPs were preserved during the polyploidization and evolutionary processes. In the synteny plotter, OGPs of *G. max* and *G. soja* were mostly found on the corresponding chromosome except for OGPs present on chromosome 6, 11, and 13 as they had OGPs on chromosomes 4, 13, and 11 respectively, in *G. soja* (Fig. 5).

Expressional analysis of the MGT gene family

Transcriptome data showed that *GmMGTs were* expressed in root, nodule, shoot, stem, leaf, and flower tissues. Some of the tissues were further categorized into different classes, such as flower open and unopened, leaf symbiotic condition, leaf ammonia, root tip, symbiotic condition, lateral root, etc. The expression data showed that most of the genes showed variegated expression in different tissues. *GmMGT1*, *GmMGT*27, *GmMGT*23, *GmMGT*14, *GmMGT*18, *GmMGT*35, *GmMGT*10, *GmMGT*36, *GmMGT*1, *GmMGT*20, *GmMGT*16, *GmMGT*25, and *GmMGT*2,

Content courtesy of Springer Nature, terms of use apply. Rights reserved.

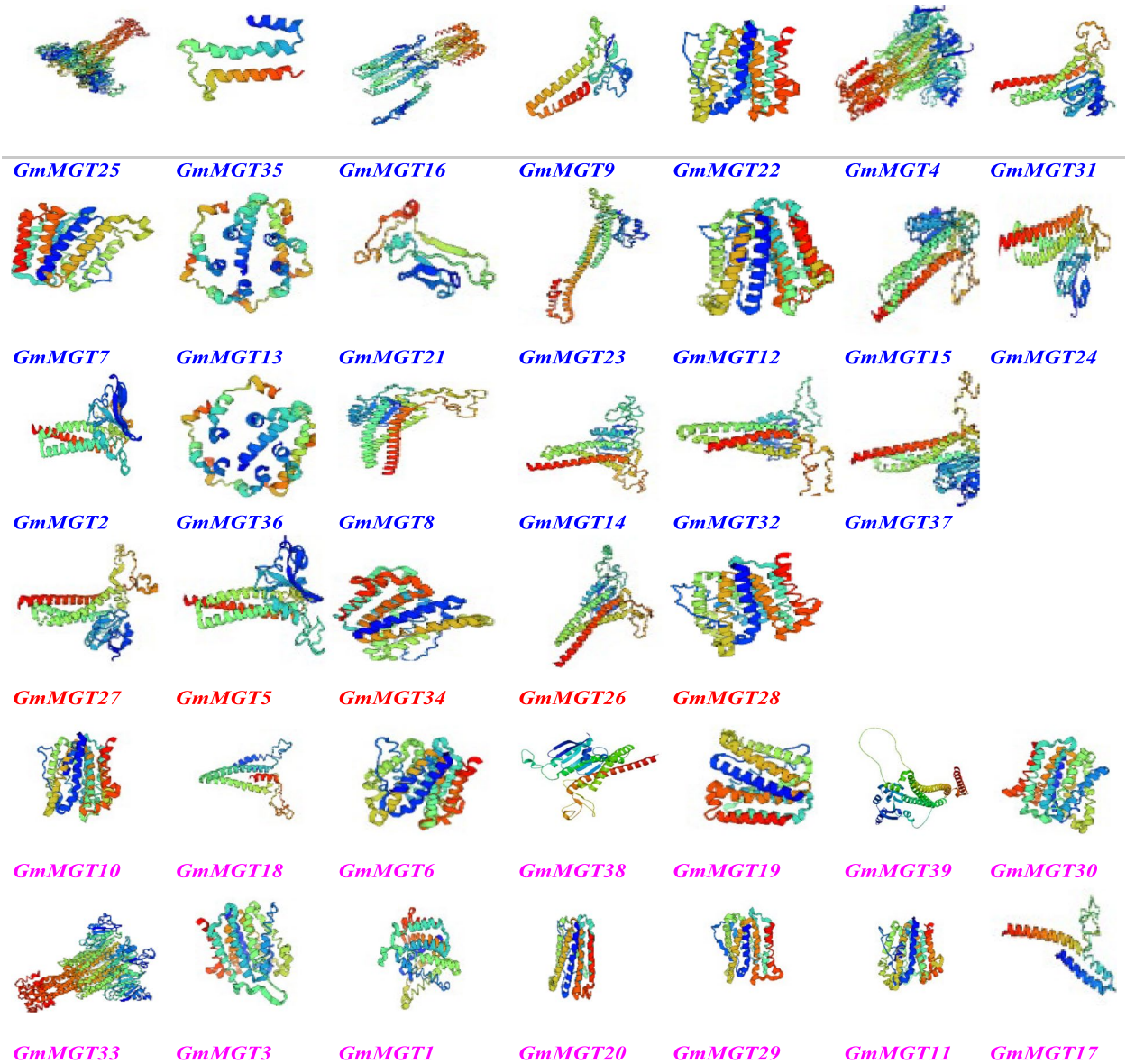

Fig. 2 Predicted 3D Protein Structure of G. max MGTs, blue color represents group NIPA, red color group CorA and purple color represents MRS/MGT

showed strong expression in all the studied tissues. However, *GmMGT*17, *GmMGT*11, *GmMGT*29, and *GmMGT*5 showed weak expression in all studied tissues. Except for *GmMGT9 and GmMGT22* which showed expression only in unopened flowers and lateral roots, *GmMGT7* and *GmMGT13* were in leaf symbiotic conditions. Most of the genes showed moderate expression in the flower open stage (Fig. 6).

Impact of Mg stress on shoot parameters

Analysis of variance showed that all the studied genotypes show significant variation for the studied shoot parameters under different Mg stress levels (Table 4). The reduction in Mg supply compared to the control showed a reduction in most of the shoot-related traits i.e., SL, SH, SFW, and SDW. Under the Mg deficiency condition (T1 = 0.01 mM) a 17.6% decrease in shoot length (35.62 cm ± 0.31) compared to the control (C) (43.21 cm ± 0.31) was recorded. The highest reduction was observed in the shoot length of the NARC-16 genotype, from 46.4 cm ± 0.90 to 33.0 cm ± 0.90 (29.0%) while the Swaat genotype showed the lowest reduction in shoot length from 43.0 cm ± 0.90 to 41.7 cm ± 0.90, with only a 2.9% reduction when the Mg supply was decreased.

Content courtesy of Springer Nature, terms of use apply. Rights reserved.

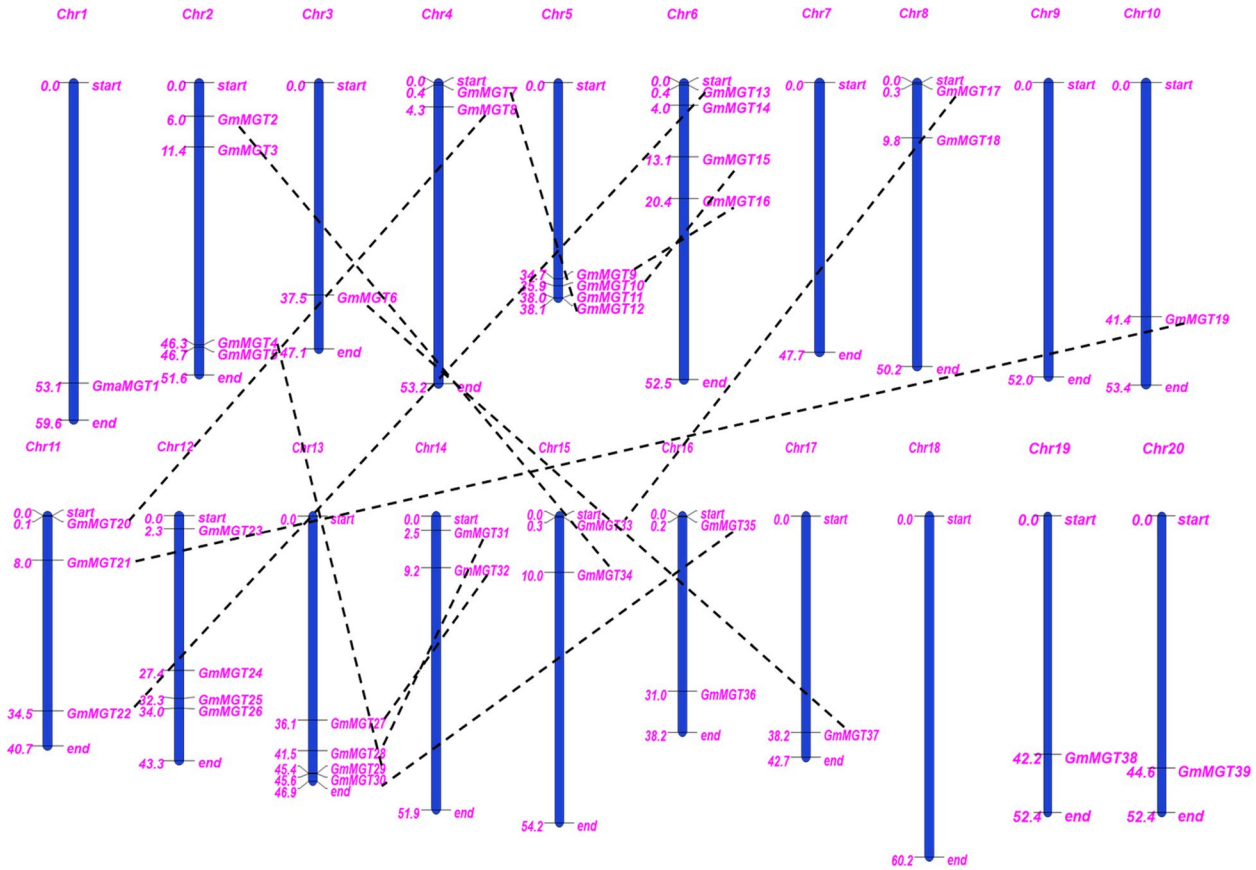

Fig. 3 Chromosomal locations and gene duplication events of MGT genes of *G. max* (blue chromosomes). The scale on the left side of the chromosome is the position of the genes in metabases', and on the right side of each chromosome, gene names correspond to the approximate locations of each MGT gene. Furthermore, the segmentally duplicated genes are connected by dashed lines represented by the black color contacting MGT Paralogues gene pairs (PGPs)

Table 2 Gene duplication analysis for the MGT gene families of *G. max*

Gene 1	Gene 2	Ka	Ks	Ka/Ks	Selection	Time (MY)	Duplicate Type
GmMGT7	*GmMGT12*	0.00	0.09	0.04	Purifying	6.93	Segmental
GmMGT19	*GmMGT21*	0.04	0.09	0.46	Purifying	6.80	Segmental
GmMGT22	*GmMGT13*	0.48	1.37	0.35	Purifying	104.64	Segmental
GmMGT4	*GmMGT29*	0.01	0.08	0.11	Purifying	6.36	Segmental
GmMGT8	*GmMGT20*	0.17	0.69	0.25	Purifying	52.92	Segmental
GmMGT2	*GmMGT34*	0.02	0.12	0.14	Purifying	8.81	Segmental
GmMGT30	*GmMGT35*	0.02	0.11	0.18	Purifying	8.17	Segmental
GmMGT17	*GmMGT33*	0.07	0.21	0.31	Purifying	16.04	Segmental
GmMGT24	*GmMGT26*	0.02	0.11	0.23	Purifying	8.03	Segmental
GmMGT9	*GmMGT16*	0.02	0.13	0.15	Purifying	10.08	Segmental
GmMGT6	*GmMGT37*	0.01	0.12	0.11	Purifying	8.92	Segmental
GmMGT28	*GmMGT31*	0.01	0.10	0.06	Purifying	7.74	Segmental
GmMGT10	*GmMGT15*	0.08	0.18	0.46	Purifying	13.48	Segmental
GmMGT27	*GmMGT32*	0.04	0.14	0.32	Purifying	10.46	Segmental

Content courtesy of Springer Nature, terms of use apply. Rights reserved.

Table 3 Description of putative cis-acting regulatory elements

Category	Motif	Function
Biotic stress	ACE	Cis-acting element involved in light responsiveness
	GT1-motif	Light responsive element
	chs-CMA1a	Part of a light responsive element
	AT1-motif	Part of a light responsive element
	GA-motif	Part of a light responsive element
	TCCC-motif	Part of a light responsive element
	GATA-motif	Part of a light responsive element
	I-box	Part of a light responsive element
	TCT-motif	Part of a light responsive element
	Gap-box	Part of a light responsive element
	Sp1	Light responsive element
	ACE	Cis-acting regulatory element involved in light responsiveness
	MRE	MYB binding site involved in light responsiveness
	Box 4	Part of a conserved DNA module involved in light responsiveness
	ATC-motif	Part of a conserved DNA module involved in light responsiveness
	ATCT-motif	Part of a conserved DNA module involved in light responsiveness
	AE-box	Part of a module for light response
	G-Box	Cis-acting regulatory element involved in light responsiveness
	ARE	Cis-acting regulatory element essential for the anaerobic induction
	LTR	Cis-acting element involved in low-temperature responsiveness
	MBS	MYB binding site involved in drought-inducibility
	TC-rich repeat	Cis-acting element involved in defense and stress responsiveness
Phytohormones	CGTCA-motif	Cis-acting regulatory element involved in the meja-responsiveness
	TGACG-motif	Cis-acting regulatory element involved in the meja-responsiveness
	TCA-element	Cis-acting element involved in salicylic acid responsiveness
	GARE-motif	Gibberellin-responsive element
	P-box	Gibberellin-responsive element
	ABRE	Cis-acting element involved in the abscisic acid responsiveness
	TGA-element	Auxin-responsive element
Growth and Development	GCN4_motif	Cis-regulatory element involved in endosperm expression
	CAT-box	Cis-acting regulatory element related to meristem expression
	Circadian	Cis-acting regulatory element involved in circadian control
	O2-site	Cis-acting regulatory element involved in zein metabolism regulation

The shoot length of plants supplied with 10 mM Mg also showed a reduction (38.30 cm ± 0.31) from the control (43.21 cm ± 0.31), hence an 11.4% reduction from the control. When the Mg supply was increased/ surplus, the highest reduction was observed in the shoot length of the Malakand-91 genotype, from 37.15 cm ± 0.90 to 28.70 cm ± 0.90 (29.0%) while genotype Swaat still showed the lowest reduction in shoot length from 43.0 cm ± 0.90 to 42.25 cm ± 0.90, with only a 1.6% reduction (Fig. 7).

Similarly, a reduction of 16.7% in seedling height under Mg deficient conditions and 9.4% under surplus conditions was recorded. The response of the genotypes was also highly variable. Under deficient and surplus Mg conditions, the Malakand-91 genotype showed the highest reduction from 11.35cm ± 0.84 to 8.05cm ± 0.84 (31.1%) and 19.4% respectively. Rawal showed the smallest reduction of 9.9% under Mg- deficient condition while in surplus Mg condition, AARI showed the smallest reduction in seedling height (3.5%) (Fig. 7).

Shoot fresh weight and shoot dry weight also showed a reduction under both stress conditions i.e. deficient and surplus Mg stress. In deficient Mg availability condition, a 20% reduction in SFW and 21% reduction in SDW was recorded while in surplus Mg availability, an 8% reduction in SFW and 15% reduction in SDW were observed. The Swaat genotype showed a 2.6% increase in SFW in response to surplus Mg availability over the control, while the rest of the genotypes showed a reduction

Content courtesy of Springer Nature, terms of use apply. Rights reserved.

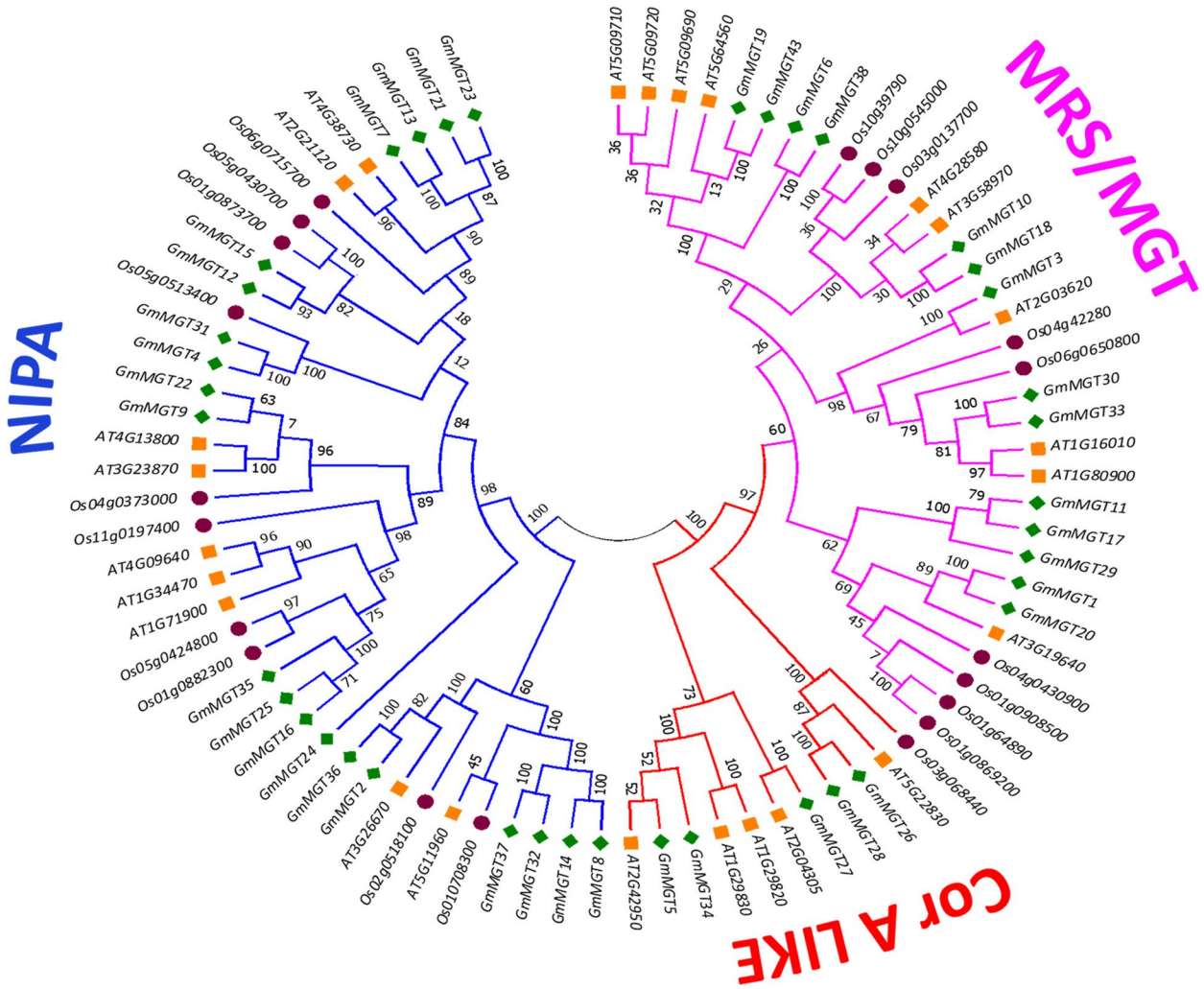

Fig. 4 Phylogenic tree of MGT proteins. The tree was constructed in MEGA 7 using the neighbor-joining method with 1000 bootstraps. Different clades of trees are marked with different colors of branch lines: Clade I (purple) MRS/MIT Type, Clade II (red) CorA and Clade III (Blue) NIPA

in SFW as well as SDW in both Mg concentrations over control (Fig. 7).

Impact of Mg stress on root parameters

Analysis of variance showed that all the genotypes showed significant variation for the studied root parameters under different Mg stress levels (Table 4). Mean comparison of genotypes × Mg levels by LSD test showed different grouping among them showing significant interaction among genotypes and Mg levels (Additional file 4). Root parameters including RL, RFW, and RDW were reduced as compared to control under both Mg stress conditions (deficiency T1 = 0.01 mM and surplus T2 = 10 mM). However, in the Mg deficiency condition, the reduction was high as compared to the high availability of Mg for these parameters. A 17.6% decrease in root length (9.77 cm ± 0.223, 21.0% decrease in root fresh weight (0.21 mg ± 0.003), and 38.5% decrease in root dry weight (0.03 mg ± 0.0006) compared to root length (11.86 cm ± 0.22), root fresh weight (0.26 mg ± 0.003) and root dry weight 0.04 mg ± 0.0006 in control were observed under low Mg condition. When Mg availability increased/surplus a 3.1% decrease in root length (11.49 cm ± 0.22), 11.7% decrease in root fresh weight (0.23 mg ± 0.003), and 13.7% decrease in root dry weight (0.03 mg ± 0.0006) compared to root length (11.86 cm ± 0.22), root fresh weight (0.26 mg ± 0.003) and root dry weight 0.04 mg ± 0.0006 in the control were recorded. The highest reduction was observed in the root length of the Swaat genotype which was 13.0 cm ± 0.68 to 8.75 cm ± 0.68 (32.7%) while genotype William-82 showed an increase of 47.9% in root length compared to the control (8.15 cm ± 0.68 to 12.05 cm ± 0.68) when Mg supply was

Content courtesy of Springer Nature, terms of use apply. Rights reserved.

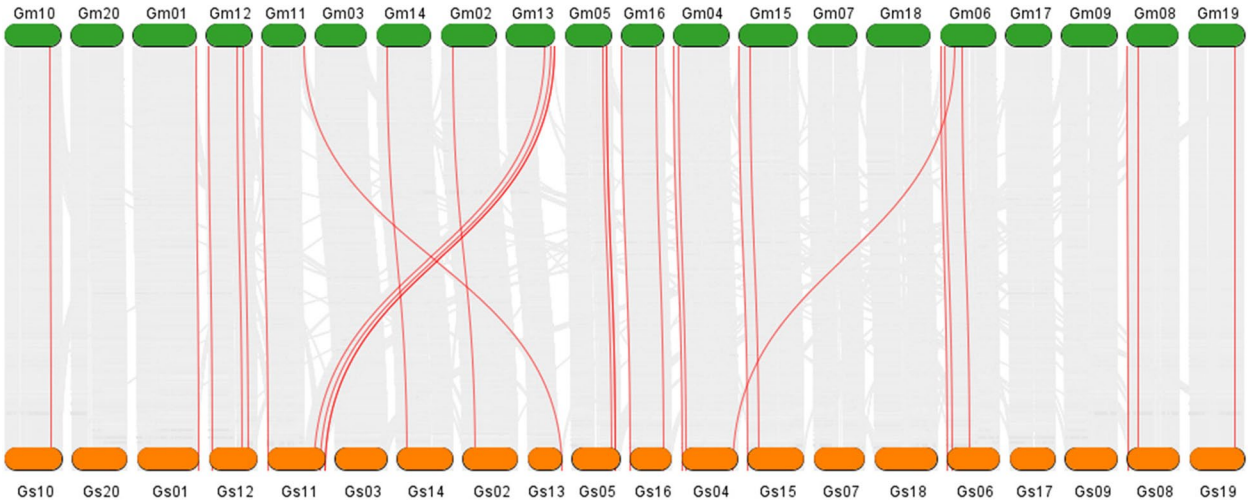

Fig. 5 Identified OGPs between G. max and G. soja genomes. A genome-scale dual-synteny plot between G. max (green boxes on the upper side) and G. soja (orange boxes on the lower side) genomes and chromosome number in green and orange boxes, respectively, with MGT genes represented by red lines

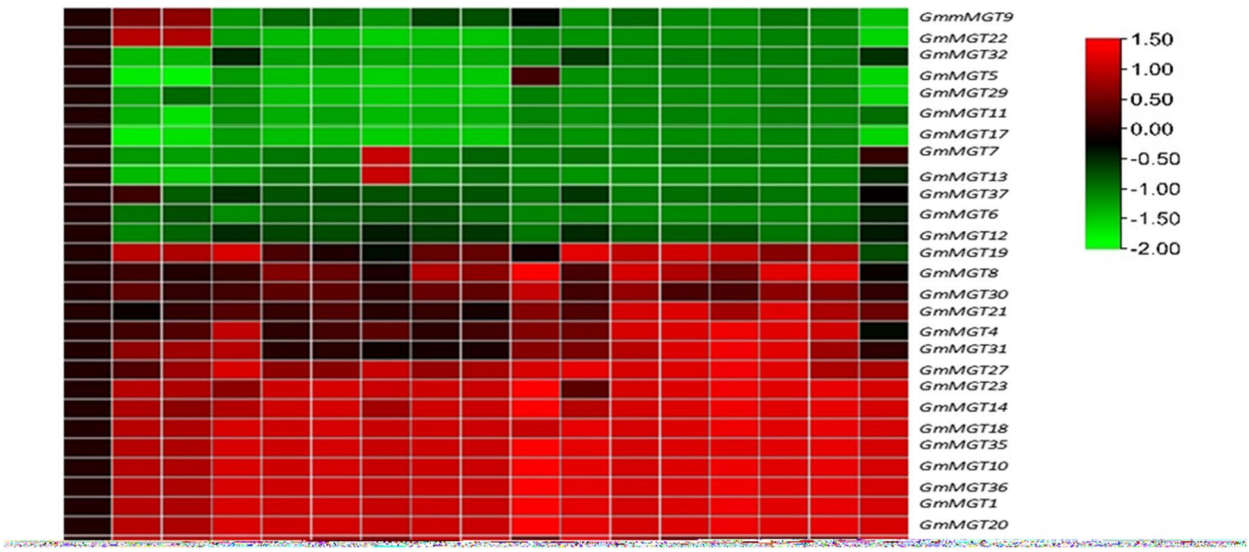

Fig. 6 Hierarchical clustering of expression profiles of G. max MGT genes in different tissues. These RNA-seq data were extracted from Phytozome

decreased. William-82 also showed an increase in root length when Mg availability was increased (13.3 cm ± 0.68) which is a 63.2% increase over control (Fig. 8).

The root shoot ratio of plants supplied with 0.01 mM Mg also showed a reduction (0.27 cm ± 0.007) from the control (0.29 cm ± 0.007), i.e., 7.8% of controls. However, when the Mg supply was increased (T2 = 10 mM), an increase of 6.6% was observed in the root shoot ratio over the control. Malakand-91, Rawal, and the William-82 genotypes showed an increase in R/S over the control (Fig. 8).

Expression Profile of Selected MGT Genes at Different Mg Levels in Soybean

For a better understanding of *GmMGT* gene functioning, their expression patterns in leaves at different hours were examined using qRT–PCRat different levels of Mg applications. For this, four genes *GmMGT2, GmMGT19, GmMGT29* and *GmMGT34* were selected based on

Content courtesy of Springer Nature, terms of use apply. Rights reserved.

Table 4 Analysis of variance for different seedling parameters of soybean genotypes under different Magnesium levels

Source	DF	Sum Square of different Studies Traits							
		SH (cm)	RL (cm)	SL (cm)	RFW (mg)	RDW (mg)	SFW (mg)	SDW	R/S
Mg level	2	741.24**	74.99**	483.41**	0.03**	0.002**	0.49**	0.010**	0.009**
Genotype	8	753.46**	27.33**	717.72**	0.01**	0.003 **	0.89**	0.007**	0.060**
Mg level x Genotype	16	176.37**	6.85 ns	161.12**	0.003*	0.00039 *	0.21**	0.002**	0.017**
Error	27	18.46	12.15	21.80	0.001	0.00020	0.04	0.0002	0.014
Total	53	1690.20	121.35	1384.14	0.045	0.00293	1.64	0.020	0.102
LSD (5%) of Mg level x Genotype		1.73	1.37	1.85	0.017	0.003	0.084	0.006	0.05

DF Degree of freedom, *SS* Sum of square, *SH* Seedling height, *RL* Root length, *SL* Shoot length (cm), *RFW* Root fresh weight, *RDW* Root dry weight, *SFW* Shoot fresh weight, *SDW* Shoot dry weight, *R/S* Root and shoot ratio

* significant at $P < 0.01$

** highly significant at $P = 0.000$

ns Nonsignificant at $P > 0.05$

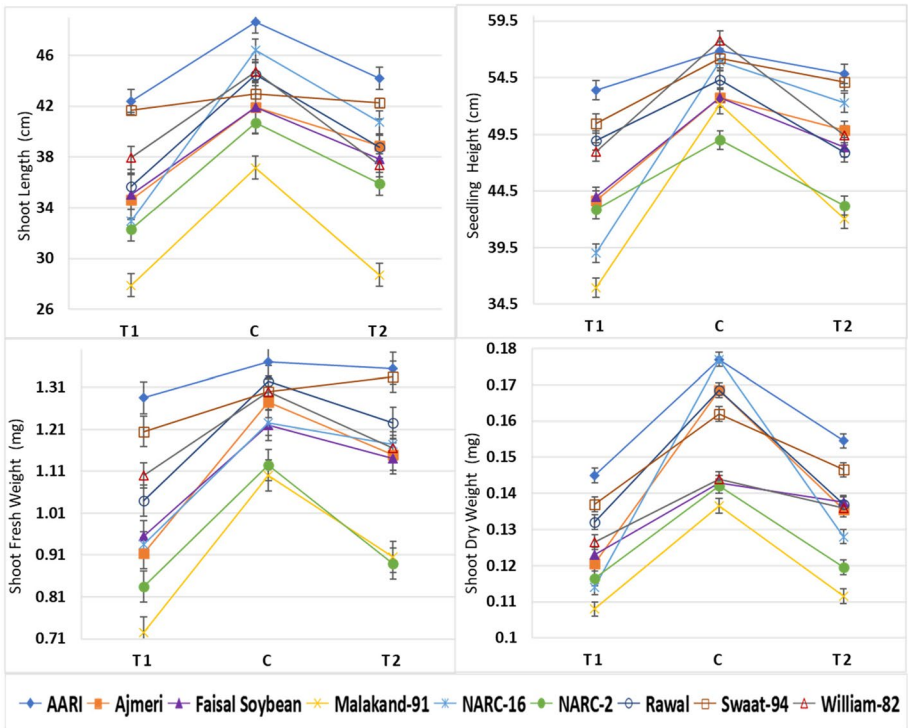

Fig. 7 Interaction plots showing significant interaction between nine soybean genotypes and 3 different Mg levels (T1 = 0.01 mM, C = 1 mM, T2 = 10 mM) for shoot related parameters i.e., Shoot length (SL), Seedling height (SH), Shoot fresh weight (SFW), Shoot dry weight (SDW)

expression data extracted from Phytozome. *GmMGT2* was selected because it reported the highest expression in all six tissues while *GmMGT29* was selected because it reported the lowest expression in all the studied tissues except flower open while GMMGT19 and GmMGT34 showed variegated expressions in all the studied tissues (Fig. 6).

All the genes showed positive qRT–PCR results while the expression of these genes was not the same at different hours in different genotypes. Under control conditions, *GmMGT2* was upregulated in AARI genotype at 3 h and gradually decreased at 6 h and 12 h while the rest of the genotypes showed a mild upregulation with an increase in time duration from 3 h to12 h (Fig. 9).

At T1 = 0.01 mM, the expression of *GmMGT19 continuously* increased in the Malakand-91 genotype from 0 to 6 h while in the Faisal Soybean *GmMGT19* expression was continuously increased from 0 to 12 h.

Content courtesy of Springer Nature, terms of use apply. Rights reserved.

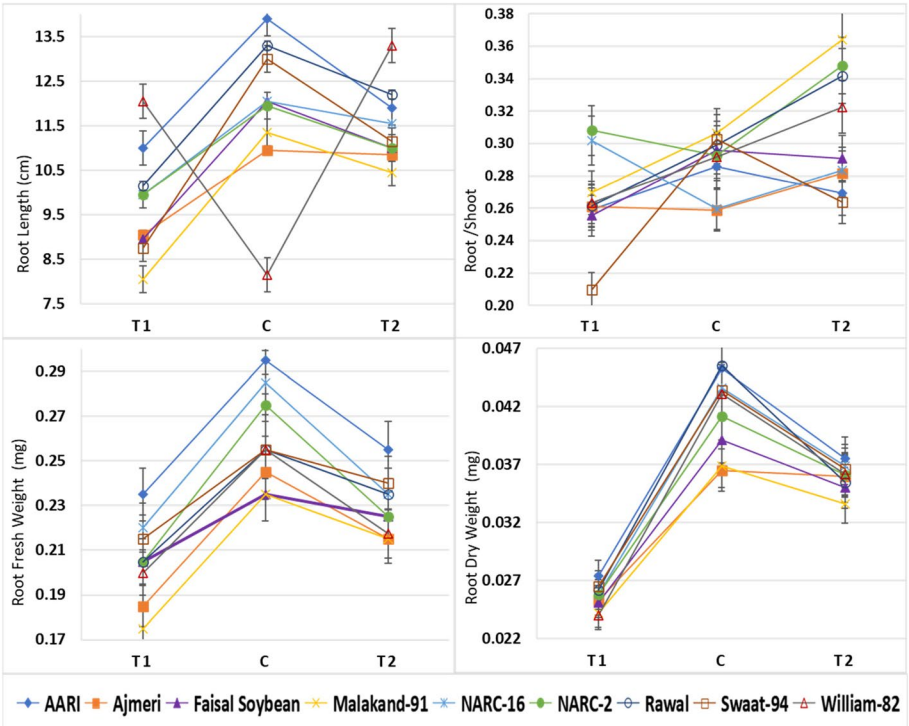

Fig. 8 Interaction plots showing significant interaction among nine soybean genotypes and 3 different Mg levels (T1 = 0.01 mM, C = 1 mM, T2 = 10 mM) for root related parameters i.e., Root length (RL), Root\Shoot ratio (R/S), Root fresh weight (RFW), Root dry weight (RDW)

At T2 = 10 mM, when Mg supplied increased from control, the expression of *GmMGT19* was upregulated in Faisal soybean genotype at 3 h while continuous increase up to 6 h was observed in Malakand-91 (Fig. 9). The AARI genotype showed highest expression of *GmMGT19* in controls at 3 h.

GmMGT29 also showed highly variable expression in response to Mg deficiency as well as surplus stress at different hours. The expression of *GmMGT29* was upregulated under Mg deficient conditions at 6 h in the Malakand-91 and Faisal Soybean while the AARI genotype showed the highest expression of *GmMGT29* gene at 12 h. At T2 when Mg was high, *GmMGT29* was upregulated continuously at 3 h and 6 h in Malakand-91 genotype while in the Faisal Soybean, it showed upregulation at 6 h. In AARI, *GmMGT29* was upregulated at 12 h as compared to the control (Fig. 9).

At T1 = 0.01 mM, the expression *GmMGT34* continuously increased in the Malakand-91 genotype from 0 to 12 h while in the Faisal Soybean *GmMGT34* expression was highest at 3 h with T2 treatment. The AARI genotype showed highest expression of *GmMGT34* in controls at 12 h when exposed to surplus Mg stress.

Discussion

Magnesium is involved in the conformational stabilization of many macromolecules such as proteins, nucleic acids, cell walls, and cell membranes [26], and also maintains many enzymatic activities, such as polymerase, ATPase, ribulose-1,5-bisphosphate carboxylase/oxygenase (Rubisco) and kinases [27]. However, Mg deficiency adversely affects the growth of plants by limiting shoot and root growth, which weakens the vascular tissue that limits water and nutrient uptake [23]. The structure and membranes of the grana are also disturbed by magnesium shortage [28]. Numerous investigations on various plant species have found that Mg shortages significantly reduce net CO_2 assimilation [5].

The Mg^{2+} transporter gene family (CorA/MRS2/MGT) has been identified in the model plant Arabidopsis [13]. To the best of our knowledge, there are no reports of the MRS2/MGT gene family in soybean. However, several gene families i.e., APX [29], CAT [29], SOD [30], GPX [30], GDSL [31], GRAS [32], BES1 [33], Hsf [34], and metal tolerance protein (MTP) [35] were identified and characterized in soybean after the completion of the soybean genome sequencing project. In this study,

Content courtesy of Springer Nature, terms of use apply. Rights reserved.

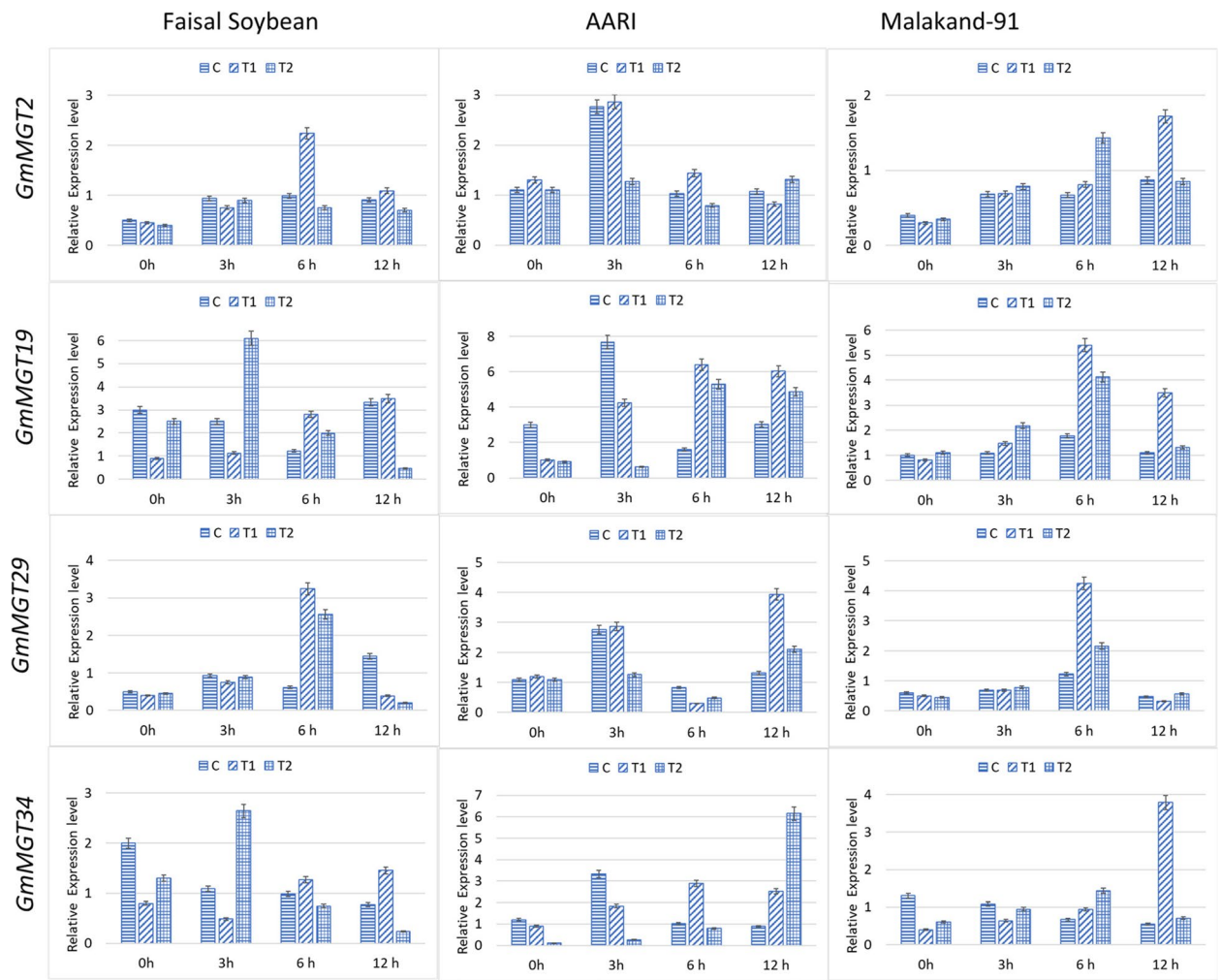

Fig. 9 Expression pattern of selected GmMGTs (*GmMGT2, GmMGT19, GmMGT29, GmMGT34*) of *G. max* under different levels of Mg treatments Control = 1 mM, T1 = 0.01 mM and T2 = 10 Mm in different soybean genotypes (Malakand, Faisal, and AARI). Data depict the mean and error bars represent the standard deviation of nine replicates ($n = 9$). At T1 = 0.01 mM when Mg was deficient, the expression of *GmMGT2* continuously increased in the Malakand-91 genotype from 6 to 12 h while in the Faisal Soybean high *GmMGT2* expression was observed at 6 h. At T2 = 10 mM, when Mg supplied increased from control, the expression of *GmMGT2* was upregulated in Malakand-91 genotype at 3 h as well at 6 h (Fig. 9). The AARI genotype showed a consistent expression of *GmMGT2* in both controls as well as deficient conditions at 3 h

the identification and characterization of the MRS2/MGT gene family in soybean were reported. In the current study, 39 MGT genes were identified in soybean. The soybean MRS2/MGT family is expanded when compared with Arabidopsis, rice and maize which have 10,11 and 12 members respectively [11–13]. Expansion in MGT gene family members as compared to model plants has also been reported in other species also such as 36 genes in Brassica napus [15], 24 genes in wheat [17] 62 genes in *C. sativa,* and 41 genes in *T. turgidum* [20]. This increase in gene numbers is predicted to be relegated to the genome size and ploidy level of a species [36]. Further genome duplication was also predicted as a major force in the expansion of gene families [37].

Phylogenetic analysis is an important tool to determine the diversity and relationships between organisms and genes, as well as to predict the evolutionary history of organisms. The evolutionary study revealed that the MGT members from *G. max, A. thaliana,* and *O. sativa* were evenly classified into 3 subfamilies, CorA, MRS2/MGT, and NIPA. Similar results of MGT classification were also observed in wheat [36]. Group MRS/MGT and NIPA showed more extension in *G. max* during the evolution as the number of the MRS2/MGT and NIPA was higher in *G. max* than CorA. This expansion may be due to a series of doublings that may have occurred in recent eras in the MRS2/MGT and NIPA subfamilies. These results may be supported by comparing the

Content courtesy of Springer Nature, terms of use apply. Rights reserved.

GmMGT gene position in the phylogenetic tree with model plant (Arabidopsis and rice) MGTs as prescribed by [16]. According to [16], *GmMGT10* and *GmMGT18* were supposed to have originated in the second round of gene duplication while *GmMGT19, GmMGT43, GmMGT6,* and *GmMGT38* were retained from the third round, and *GmMGT*30 and *GmMGT*33 were duplicated in 4th round of gene duplication in angiosperms before the split of dicots and monocots. *GmMGT11*, *GmMGT*17, *GmMGT*29, *GmMGT*01, and *GmMGT20* were derived from the ρWGD events. The CorA seemed to be more conserved than both MRS/MGT and NIPA in *G. max*. *GmMGT26* and *GmMGT28* present in CorA belong to the older group of the MGT families as both were retained from the first round of gene duplication in angiosperms as genes of model plant species *AT5G22830* and *Os03g068440* present in this clade were identified as genes that were duplicated in the first round by [16]. Furthermore, both these *GmMGT* genes were speculated to have more events for intron gain making them evolve earlier according to the 'introns-early' theory during the lengthy evolutionary process [38].

Furthermore, these identified *GmMGT* genes were not distributed evenly on chromosomes in *G. max*. The uneven distribution of *GmMGT* on each chromosome, as observed in this study, is consistent with the findings in other crops, such as sugarcane [16] and *Brassica napus* [15]. These uneven distributions of MGT genes may be the result of years of genomic evolution which caused chromosomes to shift in genes and gene location.

Gene duplication is the principal feature in plant evolution and ultimately leads to gene family expansion. It may occur at single gene or whole genome level. Single gene duplication is further classified into four models: proximal duplication, tandem duplication, transposed duplication, and dispersed duplication [37]. Since the dawn of life, several new genes have evolved through the gene duplication process. The current study also suggested that gene duplication might play an important role in the amplification of *GmMGT* gene family members in the soybean genome. Our investigation revealed that segmental duplication played a key role in the expansion of *GmMGT* genes. Ka/Ks < 1 showed that purifying selection is the major selection force of the PGPs of MGTs in soybean. Furthermore, the approximate divergence time between the duplication events showed that duplication events in *GmMGTs* occurred between 6.36 to 104.64 million years ago (MYA). Duplication of *GmMGT22/GmMGT13* occurred almost 104.64 MYA, while the recently duplicated PGP of MGT in *G. max* was *GmMGT4/GmMGT29.*

The NIPA, MRS2, and CorA proteins share a conserved domain with parallel α-helices, revealing similarities in metal ion and Mg^{2+} binding centers and catalytic sites. However, sequence variations suggest distinct roles in trans-membrane transport, adapting to diverse environmental conditions [20]. Cis-regulatory elements are important and play a crucial role in gene expression. MGT genes mostly react to a variety of stresses, including those caused by hormones, growth, and development, and biotic and abiotic stresses [17]. Multiple types of cis-elements predicted in the promoter region of MGTs of *G. max* are responsible for their involvement in biotic and abiotic stress, phytohormones, and growth and development.

The expression pattern of all *GmMGT* genes showed diversity in six tissues of plants. *GmMGT9* and 22 showed expression only in unopened flowers and lateral roots while *GmMGT7* and GmMGT13 were expressed in leaf symbiotic conditions. *GmMGT*1, *GmMGT*27, *GmMGT*23, *GmMGT*14, *GmMGT*18, *GmMGT*35, *GmMGT*10, *Gm MGT*36, *GmMGT*1, *GmMGT*20, *GmMGT*16, *GmMGT*25, and *GmMGT* 2 exhibited robust expression across all the examined tissues. This tissue-specific expression pattern underscores the significance of *GmMGT* family genes in governing the distribution of Mg in various tissues. Genes displaying specific expression in particular tissues hold potential for future investigations concerning their utilization in genetic engineering studies. These results also indicated the functional conservation and divergence of the *GmMGT* gene family as compared to the MGT gene families of Arabidopsis and rice where this family shows a constitutive expression pattern [11, 12].

Mg is the central atom of chlorophyll. It plays a vital role in photosynthesis, so Mg deficiency causes chlorophyll shortage which results in deprived and stunted growth. Chlorosis and yellowish spots on leaves are the symptoms of Mg deficiency which first occur in older leaves followed by young leaves [6]. In many studies, Mg stress affects the root development of plants [5]. Under Mg-deficient conditions, root hair becomes thin with less root hair formation and stunted root growth [23]. In our studies, *Glycine max* plants were grown under Mg surplus and Mg deficient conditions to assess their Mg absorbance and translocation power. The plants under the Mg deficiency showed chlorosis of leaves along with stunted growth as compared to normal plants. Further decreases in shoot length, root length, shoot height, root/shoot ratio, shoot and root fresh and dry weight were observed. The plants under the Mg surplus conditions did not show any sign of chlorosis and their roots were thick, had more root hairs and good root length while roots and root hair became very thin and showed poor root growth under deficient conditions. However, a decrease in vegetative parameters (shoot length, root length, shoot height, shoot, and root fresh and dry weight

Content courtesy of Springer Nature, terms of use apply. Rights reserved.

was observed under surplus Mg conditions as compared to normal conditions (C = 1 mM). However, this decrease in surplus Mg condition (T2 = 10 mM) was less than that in deficient condition (T1 = 0.01 mM). Consequently, the 1 mM Mg treatment is likely found to be sufficient to support normal growth, whereas the 10 mM Mg condition appears to be an excessive concentration for photosynthesis and leaf growth in soybean. Additionally, notable variations in vegetative responses were observed among the studied genotypes when exposed to both excess and normal concentrations of Mg. Compared with Mg normal conditions, the shoot and root parameters of Mg-susceptible genotypes i.e., NARC-16, Malakand-91, were reduced under Mg surplus as well as limitation condition, while that of Mg-tolerant genotype, i.e., AARI, did not vary between treatments. It was suggested that AARI was more tolerant to Mg surplus as well as deficiency and that it may uptake and transport Mg^{2+} more efficiently from the root to the shoot than susceptible genotypes. In our experiment, we found similar results supported by the previous study [39].

Magnesium deficiency and surplus have been reported to affect *MGT* gene expression [18, 39] so we analyzed the expression levels of the *MGT* gene in soybean under deficiency as well as surplus Mg conditions. The transcription of *GmMGTs* was detected in leaves of three selected genotypes of soybean at various times and treatments. All the candidate genes were expressed in selected genotypes. However, their expression patterns varied across different treatments. In our study, *GmMGT2* expression was first low when exposed to stress, but with the increasing time, it was upregulated under the Mg deficiency as well as Mg excess in the Malakand-91 genotype. However, in genotype, AARI *GmMGT2* showed the highest expression both in the control as well under both stress conditions, suggesting that under stress conditions, *GmMGT2* may play a vital role in the uptake and translocation of Mg and make AARI tolerant to both stress conditions. Similarly, under the Mg excess condition, *GmMGT29* showed very little upregulation at 3 h and 12 h in Malakand-91, while in Faisal it was only upregulated at 6 h. In contrast, under both Mg stress, the *GmMGT29* gene is upregulated under Mg stress at 3 h and 12 h in AARI. The results suggested that under both stress and excess conditions *GmMGT* genes play an essential role in the absorption and translocation of Mg in soybean leaves as these genes are localized in plasma membrane. Yet, more investigation is needed on whether the movement of Mg goes inside or outside in leaves from other parts of the plant for a better understanding of Mg translocation in soybean under excess and stress conditions.

Conclusion

This study presents a comprehensive analysis of the MGT gene family in soybean, providing insights into their evolutionary relationships, classification, protein structures, and expression patterns under both Mg deficiency and surplus stress conditions. A total of 39 MGT genes were identified in the *G. max* genome, exhibiting sequence and expression pattern diversity. These findings shed light on the structure and function of *GmMGT* genes. Further investigation is required to determine the direction of Mg movement within leaves from other parts of the plant, providing a deeper understanding of Mg translocation in soybean under extreme conditions.

Methods

Identification, retrieval, and characterization of MGT genes in soybean

The genome, CDS, and protein files of *G. max* (Wm82.gnm4) were downloaded from Phytozome. MGT genes were retrieved using a GFF file. Further conserved domain analysis was performed using NCBI-Conserved domain database and genes having Mg domains were selected. The selected sequences were used for further analysis. We utilized the online tool ExPASy to calculate the relative molecular weight and theoretical isoelectric point of the identified MGTs. Furthermore, we predicted the subcellular localization of MGTs using CELLO v.2.5.

Phylogenetic, gene Structure, motif, and protein structure analyses

To examine the evolutionary relationship of MGT genes in *G. max* we conducted a multiple sequence alignment of their protein sequences. This alignment was performed using the Clustal Omega online tool available at EMBL-EBI. To analyze the alignment results, we employed the neighbor-joining method within the MEGA7 software, incorporating a bootstrap value of 1000 [40, 41]. To refine the final dataset, any gaps and missing data positions were eliminated. The evolutionary distance was then calculated using the Poisson correction method, as described in [45]. The distribution of introns and exons in the gene structure was analyzed using the Gene Structure Display Server web tool. To identify conserved motifs, the MEME tool was employed, and a maximum of 8 motifs were discovered using the protein sequences. To predict the 3D protein structure, the SWISS-MODEL web tool was used.

Chromosomal mapping along with gene duplication and divergence time estimation of PGPs

We obtained the positional information of the *GmMGT* genes on their respective chromosomes from the gene

Content courtesy of Springer Nature, terms of use apply. Rights reserved.

annotation file (GFF3). These positions were then visualized on the chromosome using MapChart. To analyze the synonymous (Ks) and non-synonymous (Ka) values of paralogous gene pairs (PGPs), we utilized TB tools. The Ka/Ks ratio was employed to investigate the activation of codon selection throughout evolution. Additionally, we applied $T = Ks/2\lambda$, where $\lambda = 6.1 \times 10 - 9$ for soybean, to estimate the probable time of the duplication event [42].

Cis-acting regulatory elements

The upstream 2.0 kb promoter sequences, starting from the transcription start site of the MGT genes, were extracted using TBTool. To predict potential cis-acting regulatory elements, the extracted sequences were analyzed using the PlantCARE online web tool.

Comparative phylogenetic analysis

To perform a comparative analysis, we compared the MGT genes from two species, namely *A. thaliana* and *O. sativa*, with *G. max.* The protein files of the model plant *A. thaliana* were obtained from the TAIR database, while the protein files of *O. sativa* were downloaded from the Plaza web database. Multiple sequence alignment of the MGT gene family across these species was conducted using Clustal Omega based on their protein sequences. The resulting alignment was then utilized to examine the evolutionary relationship between *G. max* MGT genes and these model plants using the neighbor-joining method in MEGA7 software, with a bootstrap value of 1000 [40, 41]. The final dataset was refined by removing gaps and positions with missing data. To calculate the evolutionary distance, we employed the Poisson correction method [45].

OGP identification in G. max and wild soybean (G. soja)

Synteny analysis of the MGT gene family was performed by utilizing the one step MCScanX package implemented in TBtools to identify OGPs. The syntenic relationship between the MGT gene family in wild and cultivated soybean was visualized using the Dual Synteny plotter tool. This tool generated an image depicting the syntenic relationships between the genes in the MGT gene family.

Expression analysis of GmMGTs in six different tissues

To conduct transcriptome analysis of GmaMGTs, the gene IDs were submitted to the RNA sequence Atlas available at Phytozome. This analysis resulted in the generation of a table containing data for six specific tissues [43]. Gene-wise expression data were normalized before creating a heatmap. This normalization process was performed using the TBtools program, which enabled the visualization of the normalized expression data in the form of a heatmap. For a deeper understanding of the MGT response under Mg stress (deficiency and surplus), we first studied the response of different soybean genotypes under different Mg levels, and then the expression of different *GmMGTs* was checked. Nine different soybean genotypes (Malakand-91, Swaat-94, NARC-16, NARC-2, Rawal, Ajmeri, Faisal Soybean, AARI, and William 82) were grown in pots filled with sand. Detail of theses genotypes is given in Additional file 2. Healthy seeds are selected based on uniformity, i.e., the same color, size, and shape. The raised seedling was then shifted in a hydroponic solution. A total of 40 uniform seedlings for each genotype were shifted in hydroponic in two replications for screening. Half-strength Hoagland solution was used as a nutrient source for proper plant growth. Three different levels of magnesium, T0 = 1 mM to represent control (C), T1 = 0.01 mM to represent deficient or stress conditions and T2 = 10 mM to represent surplus/excess were used to screen soybean genotypes. Magnesium Sulphate ($MgSO_4$) was used to prepare the solution of the desired concentration. Stress was applied to the seedling after 72 h of shifting in a hydroponic solution. The planting of soybean seedlings followed a completely randomized design (CRD), and two biological replicates were employed for the stress treatment. The pH of the solution was maintained in the range of 6.4–6.5 for proper growth of seedlings. Concentrated HCl and NaOH solutions were used for pH maintenance. An air pump was used for oxygen supply to roots in a hydroponic solution. Data were recorded for the following traits: root length, shoot length, seedling height, root/shoot ratio, fresh root weight, fresh shoot weight, dry root weight, and dry shoot weight after 12 days of seedling shifting in hydroponic solution. Data were recorded for each genotype in replication by selecting plants, and the average values were obtained for further analysis. To assess the variation in the recorded data, ANOVA was performed. The ANOVA calculations and assessment of variability among soybean genotypes were conducted using Statistix 8.1 software. To estimate the diversity among treatments, the mean comparison differences were determined using the Least Significant difference (LSD) test, which compared the mean values obtained from different treatments.

Transcript abundance analysis under Mg stress

Samples of soybean leaves from three selected genotypes (Malakand, Faisal, and AARI) were collected and stored at -80 °C in the soybean laboratory after being subjected to different magnesium (Mg) treatments. To evaluate the expression of *GmMGT* genes, the leaves were used to extract total RNA using the RNAprep Pure Plant Kit (Tiangen, Beijing, China) according to the instructions provided by the manufacturer. A Nanodrop ND-1000 spectrophotometer was

Content courtesy of Springer Nature, terms of use apply. Rights reserved.

employed to determine the purity and concentration of the total RNA, whereas RIN was assessed using an Agilent 2100 bioanalyzer. Following the manufacturer's instructions, cDNA synthesis was conducted using the Thermo Scientific RevertAid cDNA Synthesis Kit (K1622; 100 rxns). For each cDNA template, quantitative real-time PCR (RT-qPCR) was performed using Thermo Scientific Maxima SYBR Green qPCR Master Mix (2X) according to the standard protocol. The PCR amplification conditions were configured as follows: an initial denaturation step at 95 °C for 10 min, followed by 40 cycles of denaturation at 95 °C for 15 s, annealing at 60 °C for 60 s, and extension at 72 °C for 20 s in a 10 µL reaction mixture. Each sample was subjected to three biological replicates. Normalization of the PCR results was performed by utilizing the Ct value of the soybean actin gene (*Glyma.05G188800*) as an internal control. The relative expression level of each gene was determined using the $2^{\wedge-\Delta\Delta Ct}$ method [44]. All primers were generated using the gene script web tool. Primer sequences are outlined in Additional file 3.

Abbreviations

ANOVA	Analysis of variance
CDD	Conserved domain database
DSW	Dry shoot weight
DRW	Dry root weight
GFF3	Gene annotation file
FRW	Fresh root weight
FSW	Fresh shoot weight
LSD	Least significant difference
Mg	Magnesium
MGT	Magnesium Transporter
MYA	Million years ago
PGPs	Paralogous gene pairs
OGP	Orthologous gene pair
RL	Root length
RIN	RNA integrity number
SL	Shoot length
SH	Seedling height

Supplementary Information

The online version contains supplementary material available at https://doi.org/10.1186/s12870-024-05985-7.

Supplementary Material 1.

Supplementary Material 2.

Supplementary Material 3.

Supplementary Material 4.

Acknowledgements
We are thankful to the Punjab Agricultural Research Board (PARB) Project number PARB 20-350 for the financial support. The authors would like to extend their sincere appreciation to the Researchers Supporting Project number (RSP2025R194), King Saud University, Riyadh, Saudi Arabia.

Authors' contributions
MA, JAB conceived and designed the experiments. AA, JA performed the experiments. AA, JA, SA, MA, QR, MKR, IS, AI, SN, ZA, IAR, WA, MIK analyzed the data. SA, MA, AA, JA, drafted the manuscript. ARZG and MSH reviewed the manuscript and sponsored the research.

Funding
Researchers Supporting Project number (RSP2025R194), King Saud University, Riyadh, Saudi Arabia.

Data availability
All the data generated or analyzed in our study is included in this published article itself.

Declarations

Ethics approval and consent to participate
Not applicable.

Consent for publication
Not applicable.

Competing interests
The authors declare no competing interests.

Author details
[1]Department of Plant Breeding and Genetics, University of Agriculture, Faisalabad, Pakistan. [2]Barani Agricultural Research Station, FatehjangAyub Agricultural Research Institute, Faisalabad, Pakistan. [3]Department of Botany, University of Agriculture, Faisalabad, Pakistan. [4]Faculty of Agriculture and Veterinary Sciences, Superior University, Lahore, Pakistan. [5]Department of Botany and Microbiology, College of Science, King Saud University, Riyadh 11451, Saudi Arabia. [6]College of Life Sciences, University of Chinese Academy of Sciences, Beijing, China. [7]Cotton Research Station, Faisalabad, Ayub Agricultural Research Institute, Faisalabad, Pakistan. [8]Department of Environmental Sciences, University of Veterinary and Animal Sciences, Lahore, Pakistan. [9]Centre of Agricultural Biochemistry and Biotechnology (CABB), University of University of Agriculture, Faisalabad, Pakistan. [10]Zhejiang Lab, Hangzhou, China. [11]The Center for Advanced Studies in Agriculture and Food Security, University of Agriculture, Faisalabad, Pakistan. [12]Faculty of Biotechnology, October University for Modern Sciences & Arts, 6th October City, Egypt.

Received: 6 September 2023 Accepted: 17 December 2024
Published online: 22 January 2025

References

1. Chen ZC, Peng WT, Li J, Liao H. Functional dissection and transport mechanism of magnesium in plants. Semin Cell Dev Biol. 2018;74:142–52.
2. Lin DC, Nobel PS. Control of photosynthesis by Mg2+. Arch Biochem Biophys. 1971;145(2):622–32.
3. Ko YH, Hong S, Pedersen PL. Chemical mechanism of ATP synthase: magnesium plays a pivotal role in formation of the transition state where ATP is synthesized from ADP and inorganic phosphate. J Biol Chem. 1999;274(41):28853–6.
4. Tian X-Y, He D-D, Bai S, Zeng W-Z, Wang Z, Wang M, Wu L-Q, Chen Z-C. Physiological and molecular advances in magnesium nutrition of plants. Plant Soil. 2021;468:1–17.
5. Jaghdani SJ, Jahns P, Tränkner M. The impact of magnesium deficiency on photosynthesis and photoprotection in Spinacia oleracea. Plant Stress. 2021;2:100040.
6. Hauer-Jákli M, Tränkner M. Critical leaf magnesium thresholds and the impact of magnesium on plant growth and photo-oxidative defense: a systematic review and meta-analysis from 70 years of research. Front Plant Sci. 2019;10:766.
7. Wang Z, Hassan MU, Nadeem F, Wu L, Zhang F, Li X. Magnesium fertilization improves crop yield in most production systems: A meta-analysis. Front Plant Sci. 2020;10:1727.
8. Maguire ME. Magnesium transporters: properties, regulation and structure. Front Biosci. 2006;11:3149–63.
9. Kobayashi NI. Chapter 8 - An introduction to the Mg2+ transporters in plants. In: Upadhyay SK, editor. Cation Transporters in Plants. Academic Press; 2022. p. 129–46.
10. Knoop V, Groth-Malonek M, Gebert M, Eifler K, Weyand K. Transport of magnesium and other divalent cations: evolution of the 2-TM-GxN proteins in the MIT superfamily. Mol Genet Genomics. 2005;274:205–16.

Content courtesy of Springer Nature, terms of use apply. Rights reserved.

11. Li L, Tutone AF, Drummond RS, Gardner RC, Luan S. A novel family of magnesium transport genes in Arabidopsis. Plant Cell. 2001;13(12):2761–75.
12. Saito T, Kobayashi NI, Tanoi K, Iwata N, Suzuki H, Iwata R, Nakanishi TM. Expression and functional analysis of the CorA-MRS2-ALR-type magnesium transporter family in rice. Plant Cell Physiol. 2013;54(10):1673–83.
13. Schock I, Gregan J, Steinhauser S, Schweyen R, Brennicke A, Knoop V. A member of a novel Arabidopsis thaliana gene family of candidate Mg2+ ion transporters complements a yeast mitochondrial group II intron-splicing mutant. Plant J. 2000;24(4):489–501.
14. Li H, Du H, Huang K, Chen X, Liu T, Gao S, Liu H, Tang Q, Rong T, Zhang S. Identification, and Functional and Expression Analyses of the CorA/MRS2/MGT-Type Magnesium Transporter Family in Maize. Plant Cell Physiol. 2016;57(6):1153–68.
15. Zhang L, Wen A, Wu X, Pan X, Wu N, Chen X, Chen Y, Mao D, Chen L, Luan S. Molecular identification of the magnesium transport gene family in Brassica napus. Plant physiology and biochemistry : PPB. 2019;136:204–14.
16. Wang Y, Hua X, Xu J, Chen Z, Fan T, Zeng Z, Wang H, Hour A-L, Yu Q, Ming R, et al. Comparative genomics revealed the gene evolution and functional divergence of magnesium transporter families in Saccharum. BMC Genomics. 2019;20(1):83.
17. Tang Y, Yang X, Li H, Shuai Y, Chen W, Ma D, Lü Z. Uncovering the role of wheat magnesium transporter family genes in abiotic responses. Front Plant Sci. 2023;14:1078299.
18. Tong M, Liu W, He H, Hu H, Ding Y, Li X, Huang J, Yin L. Identification and functional analysis of the CorA/MGT/MRS2-type magnesium transporter in banana. PLoS ONE. 2020;15(10):e0239058.
19. Liu W, Khan S, Tong M, Hu H, Yin L, Huang J. Identification and Expression of the CorA/MRS2/ALR Type Magnesium Transporters in Tomato. Plants. 2023;12(13):2512.
20. Faraji S, Ahmadizadeh M, Heidari P. Genome-wide comparative analysis of Mg transporter gene family between Triticum turgidum and Camelina sativa. Biometals. 2021;34(3):639–60.
21. Pratap A, Gupta SK, Kumar J, Solanki R. Soybean. Technological Innovations in Major World Oil Crops. Breeding. 2012;1:293–321.
22. Ali N. Soybean processing and utilization. In: The soybean: botany, production and uses. Cabi Wallingford UK; 2010. p. 345–74.
23 Khaitov B. Effects of Rhizobium inoculation and magnesium application on growth and nodulation of soybean (Glycine max L.). J Plant Nutr. 2018;41(16):2057–68.
24. Zhang W, Liu Y, Muneer MA, Jin D, Zhang H, Cai Y, Ma C, Wang C, Chen X, Huang C. Characterization of Different Magnesium Fertilizers and Their Effect on Yield and Quality of Soybean and Pomelo. Agronomy. 2022;12(11):2693.
25. Zhenya L, Yanyan W, Degryse F, Huang C, Cuihong H, Liangquan W, Jiang R, Mclaughlin MJ, Zhang F. Magnesium-fortified phosphate fertilizers improve nutrient uptake and plant growth without reducing phosphorus availability. Pedosphere. 2022;32(5):744–51.
26. Silva IR, Smyth TJ, Israel DW, Rufty TW. Altered aluminum inhibition of soybean root elongation in the presence of magnesium. Plant Soil. 2001;230:223–30.
27. Hermans C, Johnson GN, Strasser RJ, Verbruggen N. Physiological characterisation of magnesium deficiency in sugar beet: acclimation to low magnesium differentially affects photosystems I and II. Planta. 2004;220:344–55.
28. Izawa S, Good NE. Effect of salts and electron transport on the conformation of isolated chloroplasts. II Electron microscopy Plant Physiology. 1966;41(3):544–52.
29. Aleem M, Aleem S, Sharif I, Aleem M, Shahzad R, Khan MI, Batool A, Sarwar G, Farooq J, Iqbal A. Whole-Genome Identification of APX and CAT Gene Families in Cultivated and Wild Soybeans and Their Regulatory Function in Plant Development and Stress Response. Antioxidants. 2022;11(8):1626.
30. Aleem M, Aleem S, Sharif I, Wu Z, Aleem M, Tahir A, Atif RM, Cheema HMN, Shakeel A, Lei S. Characterization of SOD and GPX gene families in the soybeans in response to drought and salinity stresses. Antioxidants. 2022;11(3):460.
31. Su H-G, Zhang X-H, Wang T-T, Wei W-L, Wang Y-X, Chen J, Zhou Y-B, Chen M, Ma Y-Z, Xu Z-S. Genome-wide identification, evolution, and expression of GDSL-type esterase/lipase gene family in soybean. Front Plant Sci. 2020;11:726.
32. Wang L, Ding X, Gao Y, Yang S. Genome-wide identification and characterization of GRAS genes in soybean (Glycine max). BMC Plant Biol. 2020;20(1):1–21.
33. Li Q, Guo L, Wang H, Zhang Y, Fan C, Shen Y. In silico genome-wide identification and comprehensive characterization of the BES1 gene family in soybean. Heliyon. 2019;5(6).
34. Zhang Q, Geng J, Du Y, Zhao Q, Zhang W, Fang Q, Yin Z, Li J, Yuan X, Fan Y. Heat shock transcription factor (Hsf) gene family in common bean (Phaseolus vulgaris): Genome-wide identification, phylogeny, evolutionary expansion and expression analyses at the sprout stage under abiotic stress. BMC Plant Biol. 2022;22(1):1–15.
35. El-Sappah AH, Abbas M, Rather SA, Wani SH, Soaud N, Noor Z, Qiulan H, Eldomiaty AS, Mir RR, Li J. Genome-wide identification and expression analysis of metal tolerance protein (MTP) gene family in soybean (Glycine max) under heavy metal stress. Mol Biol Rep. 2023;50(4):2975–90.
36. Faraji S, Filiz E, Kazemitabar SK, Vannozzi A, Palumbo F, Barcaccia G, Heidari P. The AP2/ERF gene family in Triticum durum: genome-wide identification and expression analysis under drought and salinity stresses. Genes. 2020;11(12):1464.
37. Qiao X, Yin H, Li L, Wang R, Wu J, Wu J, Zhang S. Different Modes of Gene Duplication Show Divergent Evolutionary Patterns and Contribute Differently to the Expansion of Gene Families Involved in Important Fruit Traits in Pear (Pyrus bretschneideri). Front Plant Sci. 2018;9:161.
38. Jeffares DC, Mourier T, Penny D. The biology of intron gain and loss. Trends in genetics : TIG. 2006;22(1):16–22.
39. Liu M, Bi J, Jin C. Developmental responses of root hairs to Mg deficiency. Plant Signal Behav. 2018;13(9):e1500068.
40. Saitou N, Nei M. The neighbor-joining method: a new method for reconstructing phylogenetic trees. Mol Biol Evol. 1987;4(4):406–25.
41 Kumar S, Stecher G, Tamura K. MEGA7: molecular evolutionary genetics analysis version 7.0 for bigger datasets. Mol Biol Evol. 2016;33(7):1870–4.
42 Lynch M, Conery JS. The evolutionary fate and consequences of duplicate genes. Sci. 2000;290(5494):1151–5.
43. Severin AJ, Woody JL, Bolon YT, Joseph B, Diers BW, Farmer AD, Muehlbauer GJ, Nelson RT, Grant D, Specht JE, et al. RNA-Seq Atlas of Glycine max: a guide to the soybean transcriptome. BMC Plant Biol. 2010;10:160.
44 Livak KJ, Schmittgen TD. Analysis of relative gene expression data using real-time quantitative PCR and the 2(-Delta Delta C(T)) Method. Methods (San Diego, Calif). 2001;25(4):402–40845. Nei M; Zhang J. Evolutionary Distance: Estimation. In Encyclopedia of Life Sciences; John Wiley & Sons, Ltd: Chichester, UK, 2005.

Publisher's Note

Springer Nature remains neutral with regard to jurisdictional claims in published maps and institutional affiliations.

Content courtesy of Springer Nature, terms of use apply. Rights reserved.

Terms and Conditions

Springer Nature journal content, brought to you courtesy of Springer Nature Customer Service Center GmbH (“Springer Nature”).
Springer Nature supports a reasonable amount of sharing of research papers by authors, subscribers and authorised users (“Users”), for small-scale personal, non-commercial use provided that all copyright, trade and service marks and other proprietary notices are maintained. By accessing, sharing, receiving or otherwise using the Springer Nature journal content you agree to these terms of use (“Terms”). For these purposes, Springer Nature considers academic use (by researchers and students) to be non-commercial.
These Terms are supplementary and will apply in addition to any applicable website terms and conditions, a relevant site licence or a personal subscription. These Terms will prevail over any conflict or ambiguity with regards to the relevant terms, a site licence or a personal subscription (to the extent of the conflict or ambiguity only). For Creative Commons-licensed articles, the terms of the Creative Commons license used will apply.
We collect and use personal data to provide access to the Springer Nature journal content. We may also use these personal data internally within ResearchGate and Springer Nature and as agreed share it, in an anonymised way, for purposes of tracking, analysis and reporting. We will not otherwise disclose your personal data outside the ResearchGate or the Springer Nature group of companies unless we have your permission as detailed in the Privacy Policy.
While Users may use the Springer Nature journal content for small scale, personal non-commercial use, it is important to note that Users may not:

1. use such content for the purpose of providing other users with access on a regular or large scale basis or as a means to circumvent access control;
2. use such content where to do so would be considered a criminal or statutory offence in any jurisdiction, or gives rise to civil liability, or is otherwise unlawful;
3. falsely or misleadingly imply or suggest endorsement, approval , sponsorship, or association unless explicitly agreed to by Springer Nature in writing;
4. use bots or other automated methods to access the content or redirect messages
5. override any security feature or exclusionary protocol; or
6. share the content in order to create substitute for Springer Nature products or services or a systematic database of Springer Nature journal content.

In line with the restriction against commercial use, Springer Nature does not permit the creation of a product or service that creates revenue, royalties, rent or income from our content or its inclusion as part of a paid for service or for other commercial gain. Springer Nature journal content cannot be used for inter-library loans and librarians may not upload Springer Nature journal content on a large scale into their, or any other, institutional repository.
These terms of use are reviewed regularly and may be amended at any time. Springer Nature is not obligated to publish any information or content on this website and may remove it or features or functionality at our sole discretion, at any time with or without notice. Springer Nature may revoke this licence to you at any time and remove access to any copies of the Springer Nature journal content which have been saved.
To the fullest extent permitted by law, Springer Nature makes no warranties, representations or guarantees to Users, either express or implied with respect to the Springer nature journal content and all parties disclaim and waive any implied warranties or warranties imposed by law, including merchantability or fitness for any particular purpose.
Please note that these rights do not automatically extend to content, data or other material published by Springer Nature that may be licensed from third parties.
If you would like to use or distribute our Springer Nature journal content to a wider audience or on a regular basis or in any other manner not expressly permitted by these Terms, please contact Springer Nature at

onlineservice@springernature.com